

A Novel Approach for Improving Turbine Wheel Quality Using Eddy Current Inspection

Jack Rose, Sean Winwood

Cummins Turbo Technologies (CTT), Huddersfield, UK

June 2015

1 Abstract

Eddy current probes are used extensively in industry to detect material defects and discontinuities. However, their use in scanning turbocharger turbine wheels is limited as the probes available on the market are often impractical at scanning the complex geometry blades on these wheels.

This paper reports on the development and capability of a bespoke, flexible, eddy current array probe, for use in scanning complex geometry turbine wheels. The sensor has been designed to detect defects that have an undesirable effect on durability in the turbine wheel. These defects are predominately located in the turbine wheel blades and they may be either sub-surface or surface contacting.

The blades of the turbine wheels were scanned using the eddy current probe. Various parameters were recorded for each of the defects that were identified by eddy current inspection. Multiple complementary Non-Destructive Evaluation (NDE) methods have been utilised to validate, characterise and understand the recorded parameters of these defects. These methods included; Fluorescent Penetrant Inspection (FPI) and 3D X-ray Computed Tomography (3DXRCT).

The eddy current probe was able to identify both artificial and naturally occurring defects in the blades of the turbine wheels. The complementary NDE methods validated the sub-surface detection capability of this flexible array.

Further work is in progress to develop improvements in cast turbine wheels. This will be achieved by monitoring blade quality using the eddy current probe while undertaking various experiments to optimise the casting procedure.

2 Introduction

The turbocharger is a device fitted to engines in order to increase efficiency and power, which may also reduce emissions and fuel consumption. The turbocharger primarily consists of a turbine wheel which recycles the hot exhaust gas from an engine and drives a compressor wheel pumping a greater volume of oxygen into the engine (Figure 1).

The turbine wheel experiences temperatures exceeding 700°C and can exceed 200krpm. To manage these conditions and yet be economically produced on mass scale, the turbine wheel is manufactured using an investment cast nickel-based superalloy.

The manufacturing process introduces the inherent defects often associated with investment casting. Defects such as small casting shell inclusions are occasionally found in the turbine blades. When located in high stress concentration regions, inclusions can lead to fatigue crack initiation.

Eddy current inspection was chosen as the most appropriate method to non-destructively inspect both surface contacting and sub-surface regions of the blade that may be more sensitive to crack initiation.

Eddy current inspection utilises the electromagnetic properties of conductive materials to detect defects or flaws. In summary, this is possible as the material flaws that have a different conductivity (cracks, casting inclusions) alter induced eddy current flow. The magnetic fields generated by these modified eddy current then interact differently with the primary magnetic fields produced by the probe. This change in magnetic field affects the current in the probe and ultimately provides a readable feedback in the form of voltage and phase angle changes (1) which would be recorded using software on a voltage or impedance plane diagram.

Until relatively recently, eddy current inspection has been limited commercially by the availability of flexible array probe setups with the capability to scan complex geometry components. For this project, a bespoke flexible probe with an array of coils was designed and manufactured. The flexibility of the probe allowed the consistent contact required to scan along a complex and difficult to access blade geometry. The flexibility also helps ensure contact is maintained despite the variations in blade dimensions caused by the investment casting process. The array of coils in the probe allowed the scan to be performed across the whole area of interest in just one pass.

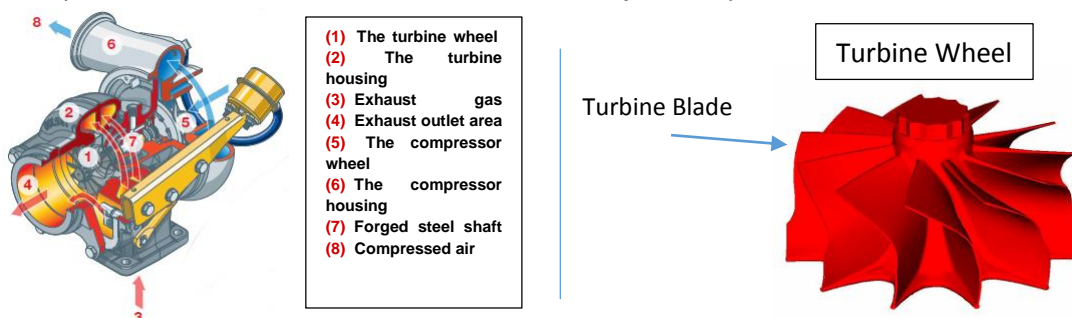


Figure 1: Left: Schematic annotated diagram of a waste-gated turbocharger (2). Right: turbine wheel schematic diagram

Figure 2 illustrates a typical turbine wheel failure due to Low Cycle Fatigue (LCF) initiating from a casting shell inclusion.

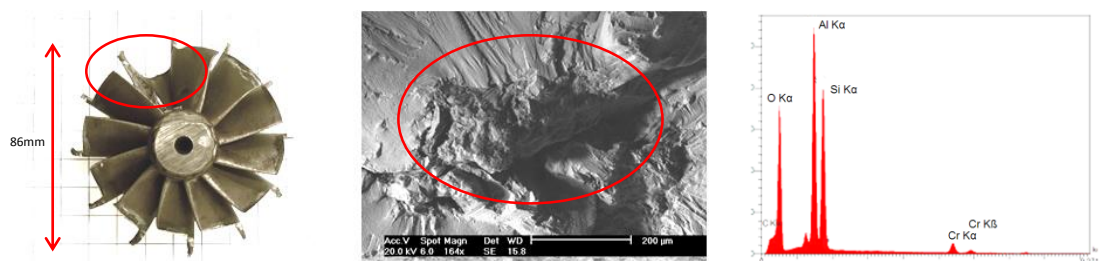


Figure 2: Example LCF failure of turbine wheel. Left: Front face of the turbine wheel showing damaged exducer. Centre: Secondary Electron SEM image of sub surface (by 100µm) inclusion measuring 300µm * 200µm in size. Right: Energy Dispersive X-ray Spectroscopy showing semi-quantitative elemental readings, showing high Al, Si and O peaks consistent with a casting shell inclusion.

The shell inclusions are aluminosilicate ceramic particles which are electrically insulating (Figure 2). Many of the inclusions may be filtered out from production through other non-destructive testing

techniques such as FPI which can detect surface contacting flaws. However, as Figure 2 illustrates, sub-surface defects can also initiate fatigue. It has been found at CTT that the inclusions are more likely to induce fatigue when between 0-250µm from the surface.

3 Experimental Procedure

The following experimental set up and procedure was followed during this investigation.

3.1 Experiment Set-Up

Figure 3 illustrates a computer aided design model of the turbine wheel, probe holder and probe.

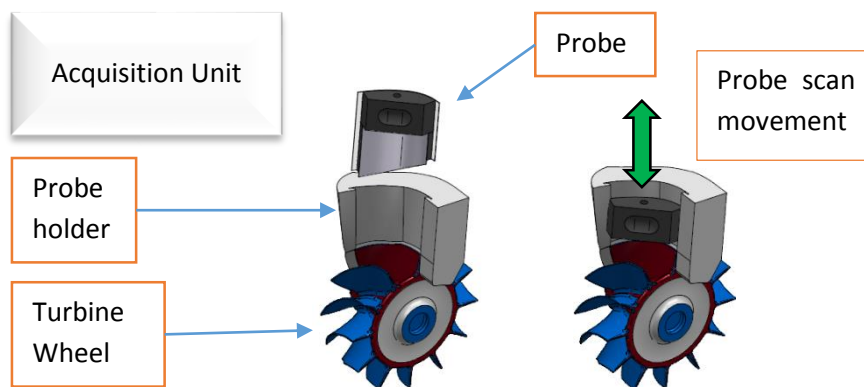


Figure 3: Schematic probe set up

3.1.1 Acquisition Unit and Software

An Eddyfi® Ectane™ E64 acquisition unit and associated Magnify™ (version 3.4R16) software package was used in this study. A multiple frequency set up was used to achieve the resolution desired at both a depth of up to 250µm and of surface contacting defects. Table 1 displays the main parameters used for the eddy current scan:

Table 1: Eddy Current Scan Parameters

Y –Axis scan speed	10mm/s
Frequency 1	500kHz
Frequency 2	300kHz

3.1.2 Probe Set up

- The probe contains 15 x 2.2mm diameter coils
- The coils are mounted onto a flexible wear resistant plastic
- The coils are organised in transmit and receive configuration with 8 coils on row 1 and 7 coils set behind in row 2.
- An additively manufactured plastic probe guide fit between the wheel blades to guide the probe along its scanning path.
- The coils are in a pancake form each with ferrite cores.

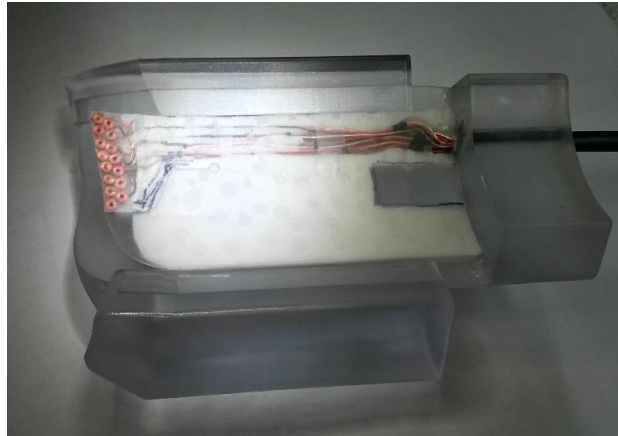


Figure 4: Photograph of bespoke flexible probe in probe holder

3.1.3 Eddy current cast and machined calibration block with Electrical-Discharge Machined (EDM) slot

The threshold levels for the defect voltage signal was set depending on the results of the scanning of two types of calibration blocks. The first calibration block consisted of both a cast and machined surface and was used in order to ensure the surface finish had little or no impact on the eddy current results (Figure 5). This calibration block was cast from the same alloy as the turbine wheel.

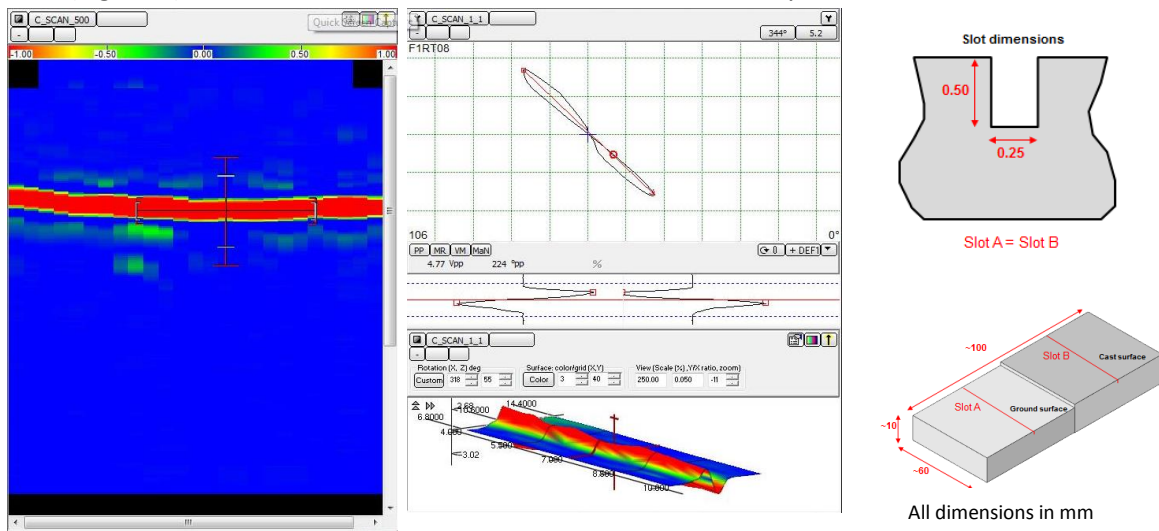


Figure 5: Calibration slot scan of EDM slot on the machined surface

3.1.4 Eddy current calibration block with defined machined holes of various depth

The second calibration block, also manufactured from the same alloy as the turbine wheel, consisted of a machined surface with a series of small holes Electrical-Discharge Machined (EDM) into the surface to a defined depth. The back of this block was then scanned to identify the depth of hole that

eddy current probe could detect. For each scan the voltages and phase angles that these created was recorded and analysed (Figure 6).

A voltage threshold of +/-0.3V was eventually selected as suitable to detect defects to the required depth of 0.25mm from the surface. Signals that exceed the threshold voltage will be highlighted by the colour red.

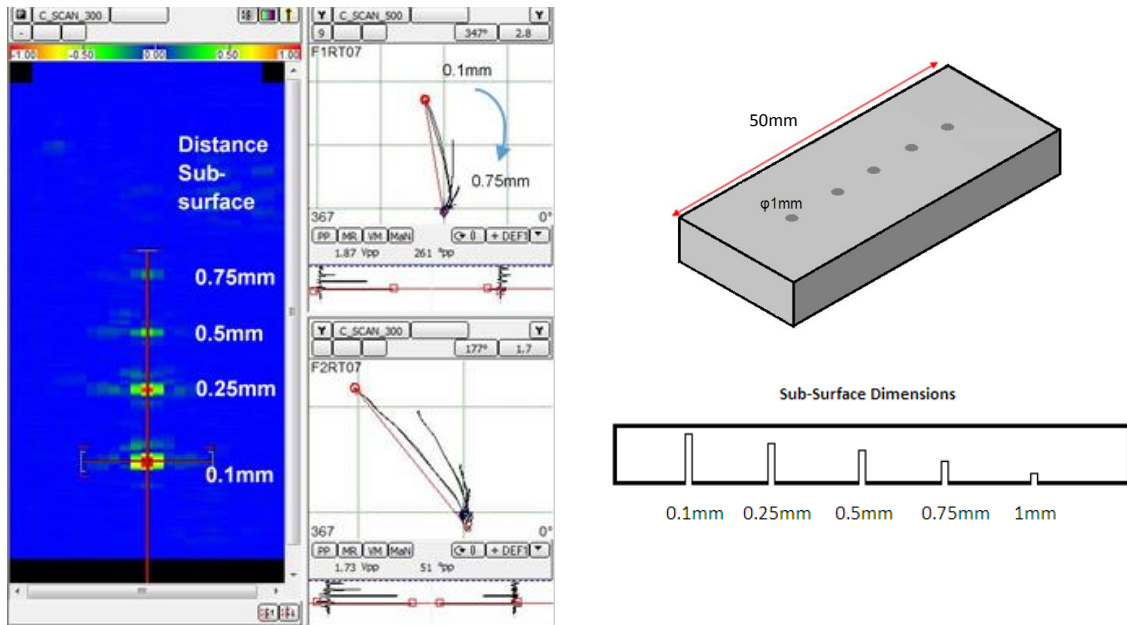


Figure 6: Reverse of calibration block with varying depths of sub-surface EDM slots.

3.1.5 3D X-ray Computer Tomography (3DXRCT)

Selected blades containing various levels of eddy current indications were machined by EDM from the wheel (Figure 7).

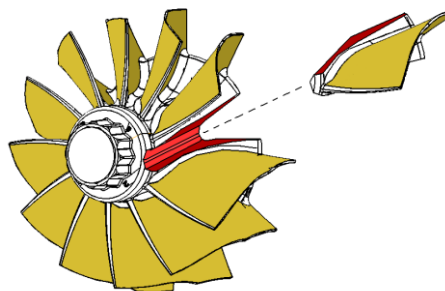


Figure 7: EDM was employed to carefully remove the blade

3DXRCT analysis was conducted on these sectioned blades to help characterise whether the defects were subsurface and understand the defect size, geometry and location. 3DXRCT was conducted on the blades with the set up shown in Table 2.

Table 2: 3DXRCT Set Up Configuration

Machine	Nikon Metrology Custom Bay 225/320kV
Target	W

Filter	Cu, 2.5 mm
Source voltage	160kV
Source power	130 μ A
Exposure time	1.415s
Number of projections	3142
Voxel size	28.6 μ m ³
Field of view	29 mm x 29 mm

3.1.6 FPI Set up

The selected blades were taken through an FPI process with the conditions set in Table 3.

Table 3: FPI Set-Up

UV Inspection Lamp	~4500 μ mW/cm ² lamp used at 300mm from source
Imaging	Digital photography, no secondary image manipulation
Fluorescent Penetrant	Chemetall Ardrex 970 P22
Developer Powder	Magnaflux Zyglo ZP-4B

4 Results

4.1 Eddy Current Results

Eddyfi acquisition software Magnifi[®] was used to capture details on defects produced. For each scan, the following details were captured:

- 1 A –scan for each frequency
- 1 colour plot c-scan with thresholds for each frequency.
- A voltage plane diagram with automated measurements to identify peak-to-peak voltage and associated phase angle

4.1.1 Typical eddy current scan without measureable defects

Two hundred wheels were used for collecting baseline measurements. Each of these wheels contain 12 blades and each of these were analysed.

Figure 8 illustrates an example of a 500 kHz frequency scan with no notable defects.

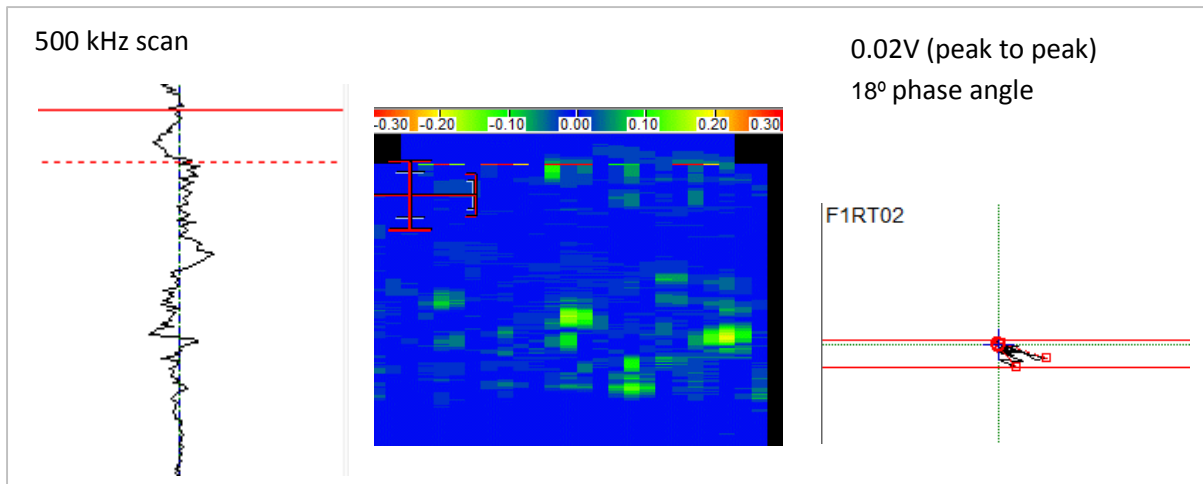


Figure 8: typical wheel scan with no known defects. Left: A-scan, Middle: C-Scan; Right: voltage plane diagram

4.1.2 Typical eddy current scan with defect detected (300 kHz and 500 kHz)

Figure 9 displays an example of a scan with a suspected defect identified by eddy current inspection. It is noted that in the 500 kHz scan, two regions that exceed the threshold level can be seen and are highlighted in red. At 300 kHz, only one region is identified having exceeding the threshold voltage.

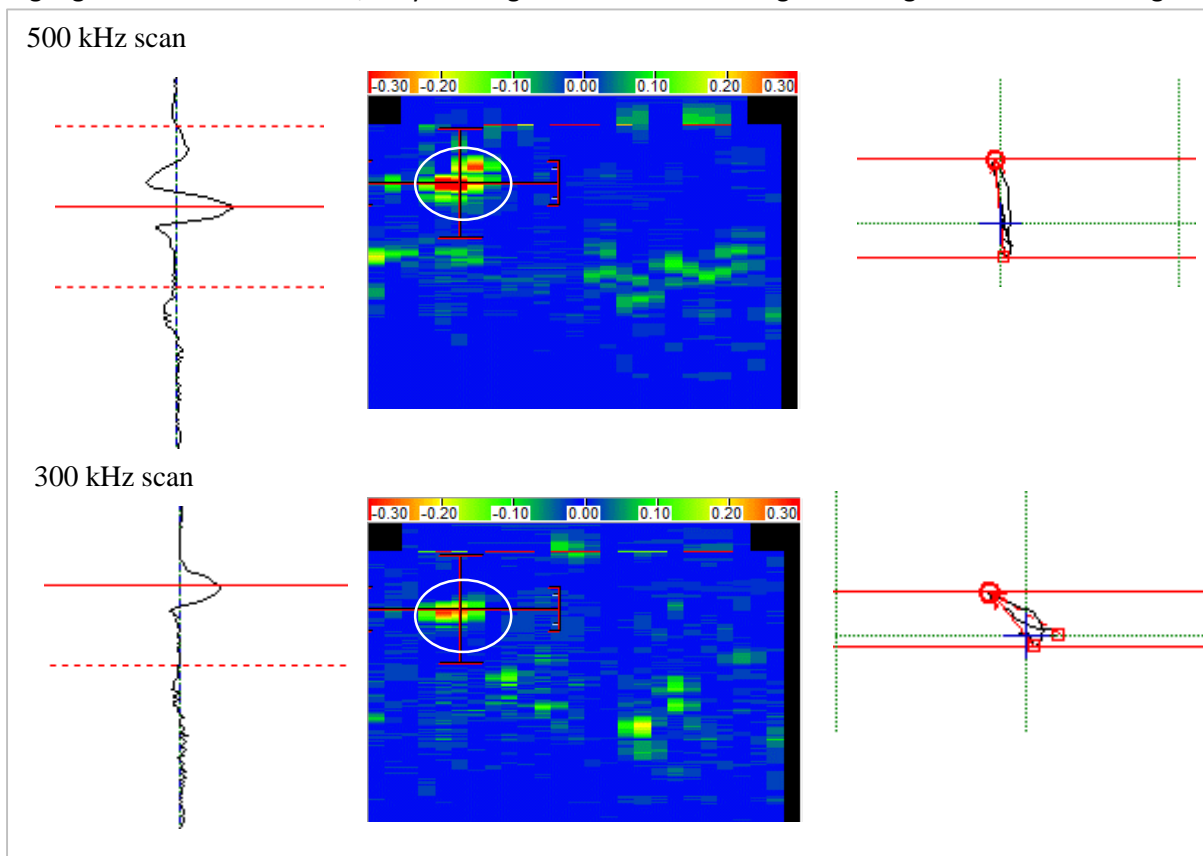


Figure 9: Typical turbine blade scan with potential defect indication

4.1.3 Example correlations between eddy current scans results with FPI and 3DXRCT

The results of the scans each of the blades were then compared to the results of the fluorescent penetrant inspection and the 3D x-ray computed tomography. An example illustrative comparison can be seen below.

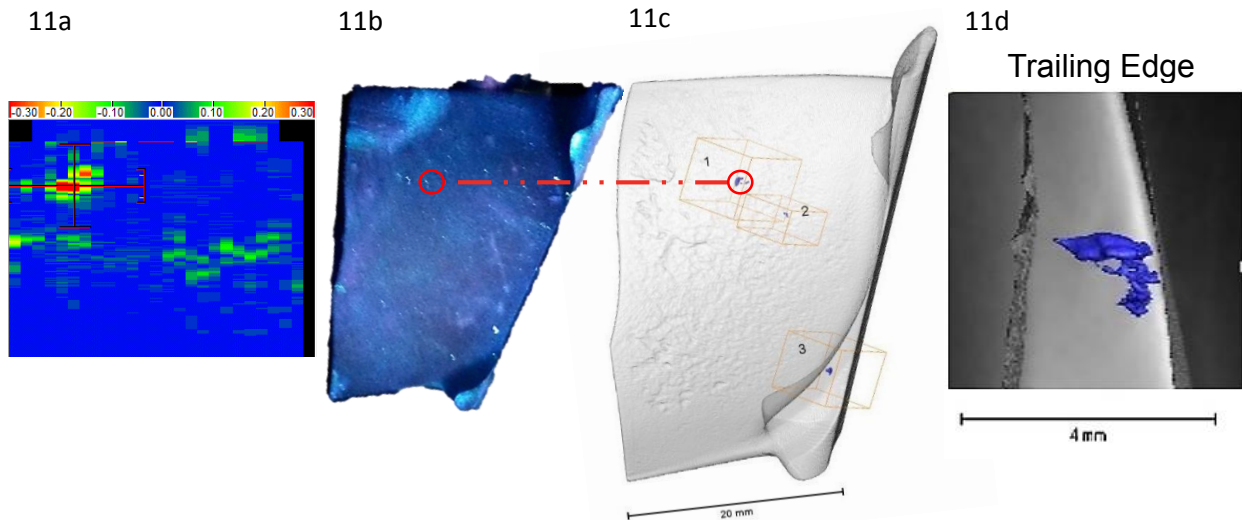


Figure 10: Correlation between Eddy Current, FPI and 3DXRCT. 11a: eddy current scan of blade. 11b: image of blade following FPI procedure with no visible bleed out. 11c: volume rendered XRCT image with defect highlighted blue. 11d: cross section of an approximately 100µm subsurface defect found through 3DXRCT.

5 Discussion

This report investigated whether flexible array eddy current technology was capable of identifying defects to a depth of 250µm from the suction surface of the turbine blade.

5.1 Calibration Procedure

Through planned calibration procedures, it was possible to ensure that the surface roughness of the scanned components had little impact on the scan results (Figure 5).

The probe also demonstrated its capability to scan a series of manufactured defects (holes) to a depth of 0.9µm from the surface, far exceeding expectations and requirements (Figure 6). It is worth noting the holes are seen as an idealised form of defect and therefore may be easier to detect than real casting shell inclusion defects.

5.2 Defect Characterisation

It is evident from Figure 9 that the eddy current system was successful in not only identifying potential defects, but also capable of giving an indication to the defect's shape by analysis of the two frequency scans. Figure 9 shows that at 500 kHz the defect is slightly elongated. At higher frequencies, it is expected due to the skin effect, the depth of penetration would be reduced and a greater resolution of near- surface characteristics would be enhanced (3). At the lower frequency of 300 kHz, the same scan showed no elongation in any direction. At 300 kHz, the eddy currents would be able to penetrate further into the blades than at the 500 kHz. This suggests that the defect was elongated in one dimension at the surface, but more cylindrical as it penetrated into the blade. The defect geometry was validated by use of 3DXRCT as demonstrated in Figure 10d.

5.3 Comparison of NDT Methods

Figure 10 also illustrates the direct comparison of the blade analyses' from FPI, 3DXRCT and ECI. The comparison of these NDT methods conclude that the defect was sub-surface. This was concluded by there being no related FPI indication in the same location, and an approximately 100µm gap apparent

in the blade cross section image from 3DXRCT. It is therefore evident that the probe is capable of detecting sub-surface defects in the region of interest.

5.4 Limitations of NDT Methods

3DXRCT was not always capable of determining surface contacting defects alone. This is because the scans often suffered from various detrimental effects such as:

- Streak artefacts such as beam hardening due to material geometry and density differences between defects and blade alloy (4)
- The nickel-base superalloy's relatively high density
- Reduced resolution when scanning small defects on a relatively large area.

This behaviour is observed in Figure 10 (centre-left) where there surface topology appears coarse and uneven which may be masking small surface-contacting defects. Figure 10d shows a variation in greyscale, where the left side of the blade is darker than the right despite being composed of the same material with the same density. This means that defects which appear as dark spots, can be missed when observing the cross sections. It also meant that it was difficult to determine the both the distance from the surface that defects were located, as well as the location where the surface of the blade physically ended because it appeared diffuse.

It was found to be fairly difficult to reproduce eddy current results without significant training and practice. This was due to the requirement to scan with a consistent speed which was difficult to maintain. This has subsequently been improved by the addition of an encoder which enables a much greater level of reproducibility.

6 Conclusions

The probe has shown that it is capable of detecting both artificial and naturally occurring defects in both surface contacting, and sub-surface locations. The probe has been capable of inspecting these defects to the required depth of 250µm from the surface.

The probe has also shown that by analysing different frequencies it is possible to build a basic understanding the defect geometry, location and depth.

Further work is currently ongoing to understand how changing casting parameters can affect the number of defects within the turbine wheel blade root. This requires close collaboration with suppliers and regular feedback of results. The aim of this is to be able to modify the casting process so as to confidently provide an improved durability turbine wheel.

7 Acknowledgements

Thanks is given to my supervisor Sean Winwood for his advice and support throughout the project, to Michael Burkinshaw, Sarah-Jane Tonks and my parents for reviewing the content of the report.

Thanks also to Aaron Greenbank and Olivier Rousseau-Cyr of Eddyfi for their support with the probe design, manufacture and software support.

Thanks is also given to the University of Manchester Henry Mosely X-Ray Imaging Facility and Julia Behnsen, and to Joseph Baptista at Avizo for their support with the x-ray computed tomography analysis.

8 References

1. **Quinn, George R.** Eddy Current Testing. [book auth.] Charles J Hellier. *Handbook of Nondestructive Evaluation*. US : McGraw-Hill, 2001, pp. 8.1-8.70.
2. **Cummins Turbo Technologies.** How a turbocharger Works. *Cummins Turbo Technologies*. [Online] 9 January 2015.
http://www.cumminsturbotechnologies.com/CTT/CTTContent/CTTUS/SiteContent/en/BinaryAsset/Images/ProductsAndTechnologies/how_a_turbo_works_diag.jpg.
3. **Rao, B P, C.** Physical Principles - 2.4.2 Skin Effect. *Practical Eddy Current Testing*. Oxford : Alpha Science International Ltd., 2007, pp. 33-35.
4. *Investigation of artefact sources in synchrotron microtomography via virtual X-ray imaging.* **Vidal, F P, et al.** 3, 2005, Nuclear Instruments and Methods in Physics Research. Section B: Beam Interactions with Materials and Atoms, Vol. 234, pp. 333-348.